A maximum noise fraction transform with improved noise estimation for hyperspectral images

4 authors, including:

Bing Zhang
University of Nevada, Las Vegas
646 PUBLICATIONS **10,612** CITATIONS

SEE PROFILE

Dongmei Chen
Queen's University
83 PUBLICATIONS **1,223** CITATIONS

SEE PROFILE

Some of the authors of this publication are also working on these related projects:

Project · vegetation parameter retrieval View project

Project · Works finished at UNLV View project

A maximum noise fraction transform with improved noise estimation for hyperspectral images

LIU Xiang[1,2†], ZHANG Bing[2], GAO LianRu[2] & CHEN DongMei[3]

[1] Institute of Remote Sensing Applications, Chinese Academy of Sciences, Beijing 100101, China;

[2] Center for Earth Observation and Digital Earth, Chinese Academy of Sciences, Beijing 100190, China;

[3] Queen's University, Kingston, ON K7L 3N6, Canada

Feature extraction is often performed to reduce spectral dimension of hyperspectral images before image classification. The maximum noise fraction (MNF) transform is one of the most commonly used spectral feature extraction methods. The spectral features in several bands of hyperspectral images are submerged by the noise. The MNF transform is advantageous over the principle component (PC) transform because it takes the noise information in the spatial domain into consideration. However, the experiments described in this paper demonstrate that classification accuracy is greatly influenced by the MNF transform when the ground objects are mixed together. The underlying mechanism of it is revealed and analyzed by mathematical theory. In order to improve the performance of classification after feature extraction when ground objects are mixed in hyperspectral images, a new MNF transform, with an improved method of estimating hyperspectral image noise covariance matrix (NCM), is presented. This improved MNF transform is applied to both the simulated data and real data. The results show that compared with the classical MNF transform, this new method enhanced the ability of feature extraction and increased classification accuracy.

principal component transform, maximum noise fraction transform, hyperspectral image, noise estimation

1 Introduction

Natural objects such as vegetation, soil and rock are often mixed with each other, and rarely in one homogenous block. Before classifying these objects from hyperspectral images, spectral feature extraction must be performed[1]. The spectral-dimension transformation methods, such as the principal component (PC) transform and maxi-mum noise fraction (MNF) transform, can be used to automatically extract the spectral features of a ground object. Many studies have applied the PC and MNF methods in hyperspectral image classification and spectral unmixing[2−5]. However, the problem of applying these two transformation methods is rarely considered, especially the impact of the spatial distribution of pixels. Obviously, the spatial distribution characteristics of ground ob-

jects vary on different hyperspectral images at different regions. For example, the crop fields are usually big and homogenous in North China and can be easily classified on images. On the contrary, the crop fields in South China are commonly mixed with different crops. This kind of mixing makes it difficult of carry out noise estimation from hyperspectral images and classification on them when there are no sensor noise statistics available. Therefore, it is necessary to study how to use spectral dimension transforms to extract features from hyperspectral images when different ground objects are mixed together.

In 1988, Green et al.[6] first presented the MNF transform method. The MNF transform generates new components ordered by image quality and provides better spectral features in major components than the PC transform method, no matter how the spectral noise is distributed. Using the theory of MNF, James et al.[7] presented the noise-adjusted principal component (NAPC) transform aiming at the noise characteristics of GER hyperspectral scanner.

The most important work in MNF transform is to accurately estimate the noise covariance matrix (NCM). There are many research papers on the developments of the NCM estimation methods and improvements of the MNF transform method[8,9]. Conradsen[10] used the SAR-model (simultaneous auto-regressive) method to estimate the NCM of images. Olsen[11] introduced five NCM estimation methods in his paper. However, all these methods only make use of the spatial characteristics of an image to estimate the NCM. Roger[12] proposed a new PC transform, called residual-scaled PC (RPC) transform, with a simple and automatic noise adjustment. The NCM in RPC is simply estimated from the image data itself through inversion of its covariance matrix. Roger indicated that RPC has near the same ability as MNF and can work rapidly like PC transform. However, unlike PC transform, the RPC method does not use the spatial characteristics of the image, and may lose useful information in the spatial domain when performing NCM estimation. Later, Roger and Arnold[13] designed a spectral and spa-

tial de-correlation (SSDC) method to estimate the noise of AVIRIS hyperspectral images. The subsequent experiments showed that this method led to noise estimation results close to those measured by sensors. Recently Gao[14] presented a method named homogeneous regions division and spectral de-correlation (HRDSDC) and successfully applied it to estimating noise for pushbroom hyperspectral imager (PHI) data. This method uses the edge detection algorithm to search the homogenous regions and combines information in the spectral dimension to estimate the noise. The result showed that it could work well for hyperspectral images covering areas with different land-cover types. However, for images with various ground objects, the homogenous regions are often too small to find. Furthermore, the main purpose of feature extraction is to classify ground objects, and the information on homogenous regions is often unknown in advance.

This paper will address the influence of the spatial distribution of samples on the results of the MNF transform. An improved MNF method is presented, in which the noise covariance matrix is estimated automatically in both the spatial and spectral domains. The new method is rarely influenced by spatial distribution of samples. The remainder of this paper is organized as follows: Section 2 introduces the basic theory of the new improved MNF transformation method. Section 3 analyzes the classification results using MNF and the new MNF method through experiments. Section 4 gives a conclusion of this study and discusses the further work with this new method.

2 Theory of methods

In this section, through the PC transform formula, we will first explain why different spatial distribution of image pixels (or called samples) cannot affect extraction results of spectral features when using PC transform. Then the impact of spatial distribution of pixels on MNF transform is explained through analysis of MNF transform formula. An improved MNF transform is presented by integrating an existing noise estimation method

LIU X et al. Sci China Ser F-Inf Sci | Sep. 2009 | vol. 52 | no. 9 | **1578-1587**

1579

on hyperspectral images with it. The reason why there is little influence from spatial distribution of samples on the new method is also addressed.

2.1 Influence of spatial arrangement of samples on PC

PC transform is a technique of transforming the original hyperspectral bands into a substantially smaller set of uncorrelated bands that represents most of information present in the original data set. It uses a principle that maximizes the variance of each band in hyperspectral images to extract principal components. Since PC transform is applied at the pixel level, the result of its feature extraction is stable, no matter how the spatial arrangement of pixels changes. MNF transform can extract the spectral features of pixels better than PC transform. However, the results of noise estimation are seriously affected by the spatial continuity of pixels. For example, when the spectral types and the numbers of ground objects to be classified are kept unchanged, and only spatial arrangement of samples is changed, MNF transform may yield different dimensionality reduction results. This will not happen in PC transform. The reason of it is analyzed below.

Assuming that a hyperspectral image has N bands, the spectral values of each pixel at different wavelengths can be treated as an N-dimensional vector x. Elements in vector x are spectral reflectance number at different wavelength bands. Assume that m is the average of vector x, namely $m = E(x)$. Covariance matrix of the image can be expressed as $\Sigma = E((x-m)(x-m)^{\mathrm{T}})$. Σ is a symmetrical and positive definite matrix.

The PC transform uses transform matrix, A, which consists of the orthonormalized eigenvectors of the covariance matrix Σ between bands. As A is symmetrical and orthogonal, i.e. $A^{-1} = A^{\mathrm{T}}$, the similarity transform of Σ by A is diagonal, i.e. $A^{-1}\Sigma A = \Lambda$. Λ is the covariance matrix of the PC-transformed image. The transformed pixel vectors, z, of the PC-transformed image are computed by $z = A^{\mathrm{T}}(x-m)$. It can be seen that A^{T} and m will keep intact when the spatial distribution of sample changes. In other words, spatial distribution of samples cannot affect the results of feature extraction of PC transform. Therefore, it is not necessary to consider the spatial information of any pixel in PC transform.

2.2 Influence of spatial arrangement of samples on MNF

In MNF or NAPC transform, eigenmatrix of Σ is no longer used as the transform matrix in the process of obtaining components ordered by signal-to-noise ratio (SNR). The transform matrix used in MNF transform is the eigenmatrix of $\Sigma\Sigma_n^{-1}$, where Σ_n is the NCM between bands. The equation for calculating generalized eigenvalue of $\Sigma\Sigma_n^{-1}$ can be expressed as $\det(\Sigma - \lambda\Sigma_n^{-1}) = 0$, where λ is the generalized eigenvalue. The information on spatial arrangement of pixels will usually be taken into account in estimating NCM of hyperspectral images. Most of the noise-estimation methods work in a spatial domain[15−17]. For example, in minimum/maximum autocorrelation factor (MAF) transform, Green et al. uses eq. (1) to obtain Σ_n:

$$\Sigma_n = \frac{1}{2}\Sigma_\Delta = \frac{1}{2}\mathrm{Cov}(x_{i,k} - x_{i+\Delta,k}), \qquad (1)$$

where Δ denotes spatial shift in vertical or horizontal orientation, e.g. $(0, 1)$, $(-1, 0)$, $(1, 1)$, etc. $x_{i,k}$ refers to the ith element in the kth band. Spatial correlation between pixels of image is used to estimate noise. Because each pixel contains the component of noise, the variance of noise gets doubled when the operation of minus is used. $1/2$ is added before covariance matrix to eliminate this influence.

In eq. (1), the subtractions between neighboring pixels must be performed in the estimating procedure of Σ_n. There are many other similar NCM estimation methods of using spatial information about pixels, such as the simple differencing method, the causal simultaneous autoregressive method, the differencing-with-the-local-mean method, the differencing-with-local-median method, and the quadratic surface method[8]. If the spatial distribution of ground objects is very complex as shown in Figure 6(a) in section 3.2 below, noise estimation results will be seriously affected. This will reduce the efficiency of spectral feature extraction using MNF transform. This influence will be tested and illustrated in the exper-

iments of section 3. In the following, an NCM estimation method which is less affected by spatial distribution of pixels is designed, and an improved MNF transform method is proposed.

2.3 MNF transform based on an improved NCM estimation method

To get the NCM of image, the noise of each pixel must be estimated. Then the standard deviation of noise in each band and covariance of noise between bands must be calculated. Since homogeneous regions cannot always be found in hyperspectral images, an NCM estimation method based on full-image process must be designed to effectively weaken the influence of the mixing of ground objects.

The method introduced in this paper uses the high spectral correlation shown in spectral signatures of hyperspectral data, which is also shown in spatial signatures. To estimate the scalar quantity value $\hat{x}_{i,j,k}$, the signal part of an original pixel $x_{i,j,k}$ at position (i,j) in the kth band, the following model which is modified from Roger and Arnold[12], can be adopted. (The planar array (i,j) is used to denote the spatial location here, which is different from eq. (1).) To consider the influences of between-band (spectral) and within-band (spatial) correlations, we estimate signal of pixel $x_{i,j,k}$ via the model:

$$\hat{x}_{i,j,k} = \begin{cases} ax_{i,j,k+1} + cx_{p,k} + d, & k = 1, \\ ax_{i,j,k-1} + bx_{i,j,k+1} \\ \quad + cx_{p,k} + d, & 1 < k < N, \\ ax_{i,j,k-1} + cx_{p,k} + d, & k = 1, \end{cases} \quad (2)$$

where

$$x_{p,k} = \begin{cases} x_{i-1,j,k}, & i > 1, \\ x_{i+1,j,k}, & i = 1, \end{cases} \quad 1 \leqslant i \leqslant W, 1 \leqslant j \leqslant H,$$

i, j and k denote the vertical, horizontal coordinates in spatial domain and band number. W, H are the width and height of the image and N is the total number of bands. The residual $r = x - \hat{x}$ is the noise estimating value of each pixel. We expect that $\Sigma r^2 = 0$ and the optimal estimation $\hat{x}_{i,j,k}$ of $x_{i,j,k}$ can be obtained with the linear regression method shown in eq. (2). The coefficients $[a\ b\ c\ d]$ are computed to minimize the noise variance of each band, that is, to minimize $S^2 = \Sigma r^2$.

There are $M = W \times H - 1$ equations that participate in the linear regression for band k. In order to get the values of these coefficients, the least square method is used to form eq. (3):

$$W \cdot [a\ b\ c\ d]' = X \Rightarrow [a\ b\ c\ d]'$$
$$= W^{\mathrm{T}}(WW^{\mathrm{T}})^{-1} \cdot X. \quad (3)$$

where X is a vector of the pixel values $x_{i,j,k}$, W is the matrix of the values of $[x_{i,j,k-1}, x_{i,j,k+1}, x_{p,k}, 1]$, k is a constant and i, j are variables. Given the coefficients of each band, the NCM of the hyperspectral image can be estimated. The variance of band k and covariance between band k and band l can be calculated by

$$\sigma_k^2 = \frac{\displaystyle\sum_{i=1}^{W}\sum_{j=1}^{H} r_{i,j,k}^2}{M - 4},$$

$$C_{kl} = \frac{\displaystyle\sum_{i=1}^{W}\sum_{j=1}^{H} r_{i,j,k} \cdot r_{i,j,l}}{M - 4}, \quad (4)$$

where $1 \leqslant k, l \leqslant N, (i,j) \neq (1,1)$. Since there are four coefficients in the linear regression, the freedom degree in the denominator is $M - 4$. Like eq. (1), formula of NCM estimation can be expressed as

$$\Sigma_n = \mathrm{Cov}(r) = \mathrm{Cov}(x_{i,j,k} - \hat{x}_{i,j,k}). \quad (5)$$

In eq. (5), since $\hat{x}_{i,j,k}$ is an unbiased estimation of the signal part in $x_{i,j,k}$, it is not necessary to divide the covariance by 2.

If the ground objects in an image are not completely mixed, the image can be divided into many blocks, and heterogeneous blocks are removed for a subsequent process. The methods shown in Roger's paper[13] and Gao's paper[14] can be used to estimate NCM for homogeneous blocks first. This improved method can be used to estimate NCM Σ_p of each block, where $1 \leqslant p \leqslant n$ and n is the number of homogeneous blocks that can be found on the image. The mean value of NCM of all blocks can be used as the NCM of the whole hyperspectral image.

It should be noted that, due to the partial use of spectral correlation in noise estimation, the results of noise estimation are also correlated. Noise

covariance C_{kl} between bands is reserved after calculating Σ_n in our method, unlike the NCM estimation method in Greco's paper[18], the higher the interval between bands (i.e., the larger the difference of k and l), the lower the C_{kl}.

In this new method, spectral correlation is used to estimate NCM when ground objects are mixed together. The correlation between pixels in the spatial domain is considered more than in the spectral domain when ground objects are not mixed. The optimal NCM estimation method of using the linear regression model makes the improved MNF transform method adaptable to the variety of correlation in spectral or spatial domain.

This transformation method requires that the spectra of pixels should be continuous, which is very common in hyperspectral images. The proposed method uses the least square algorithm to calculate four coefficients, and the cost of computation is high. Therefore, it is more suitable for hyperspectral images with a small field of view.

3 Experiments and analysis

Simulated HYMAP hyperspectral images are used to illustrate the feature extraction results of the improved MNF transform and the classical MNF transform. Later, a real hyperspectral image containing mixed ground objects is used to demonstrate the performance of the improved MNF transform method.

3.1 Analysis of the influence of mixing levels of ground objects on classification accuracy

In this experiment, six different ground objects are drawn out with different spectral vectors from the HYMAP hyperspectral image first. Three types of rocks and three types of vegetations are denoted by R1, R2, R3 and V1, V2, V3. The spectral curves of 110 samples with 115 bands from 400 to 2500 nm of each object are shown in Figure 1. It can be seen that all spectra are mixed together and hard to distinguish.

Some training samples of six classes used for supervised classification are shown in Figure 2(c). The training samples and the bands selected af-

ter MNF transform must be the same in all the tasks. To clearly simulate the real classification circumstances, less than 10% of all training samples and six feature bands of the transformed hyperspectral image are chosen in the classifications. A simple classification method, minimum euclidean distance, is used to obtain the OA data from this experiment after bands-feature selection. The six feature bands after the MNF transform are shown in Figure 2(d). It can be seen from Figure 2(d) that the OA results obtained using MNF are acceptable in this experiment. But the results using PC transform, as shown in Figure 2(e), are not acceptable. It is clear that the classical MNF transform has an obvious advantage in feature extraction when ground objects are mixed. However, the classical MNF transform seriously affects the accuracy of classification when the mixing levels of ground objects are high. This will be proved in the next experiment.

Next, we simulated images with different mixing levels of ground objects. Figure 3 shows those simulated images with different spatial arrangements of mixing blocks. The total width and height of each hyperspectral image are the same. But the level of mixing is varied. The subscript numbers in Figure 3 express the number of scattered blocks. In every experiment, it must be ensured that, no matter how the positions of samples vary, training samples are consistent. This is achieved using recursive procedure. When classifying the image, the first six principal components extracted by MNF transform are used at all times. Because the results of the minimum distance (MD) classification method are easily influenced by spatial distribution and spectral noise, this method is used in all experiments to show the ability of each transform method to restrain noise.

In each experiment, OA is used as the criterion for evaluating the performance of feature extraction. In Figure 4, the X-axis represents the number of divided blocks of the same class, the Y-axis represents the OA after using classical MNF transform, and the black dashed line and gray dashed line represent the OA with and without PC transform, respectively. It can be seen from Figure 4 that the overall accuracy of classification with and
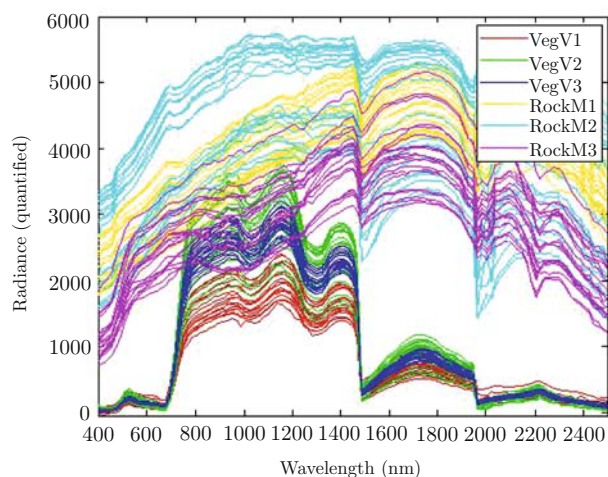
Figure 1 Sample spectral curves of six sorts of ground objects, vegetations and rocks. (The color denotations used in other figures are the same.)
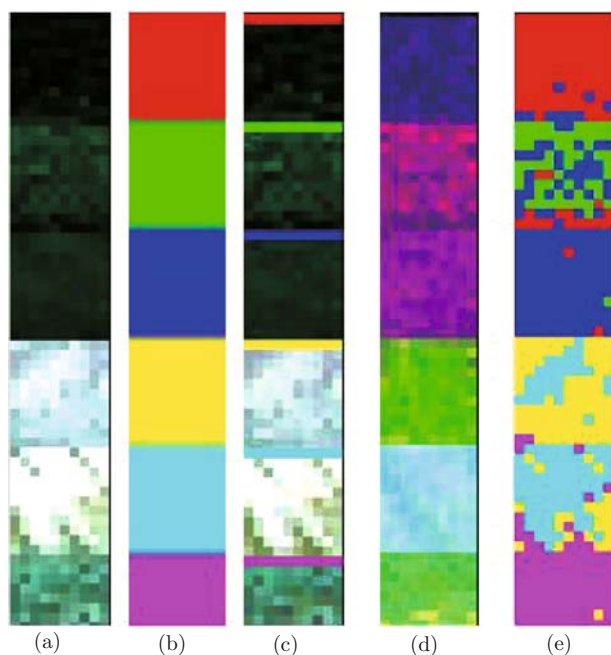
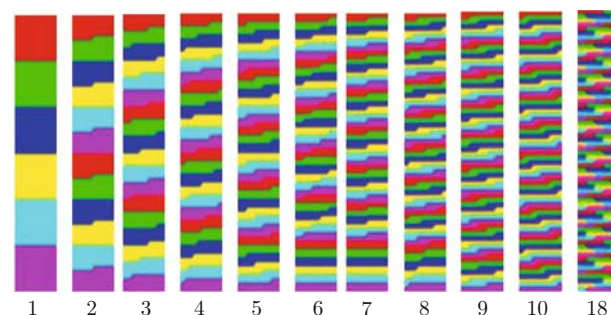ture extraction of MNF transform and classification accuracy.

Figure 3 Accurate classification maps (ground truth) when ground samples were segmented into blocks with specified number, from 1 block to 18 blocks. For paper limit, some maps (11–17 blocks) are not displayed here.
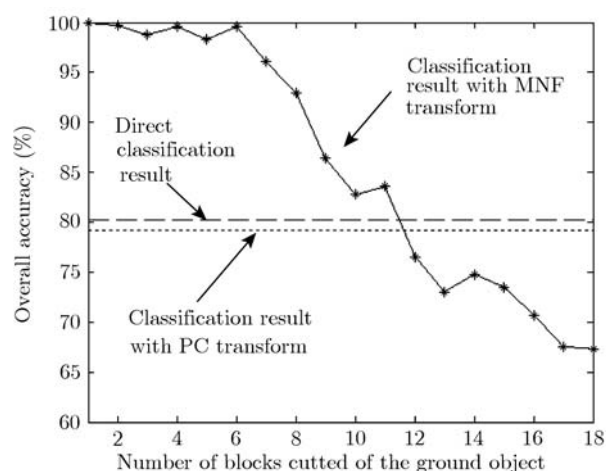

Figure 2 (a) Simulated hyperspectral image with reordered samples (R: 463 nm; G: 563 nm; B: 663 nm); (b) ground truth; (c) training samples in the image; (d) results of MNF transform (combined with the first 3 components); (e) results of classification with PC transform.

Figure 4 The classification accuracy values of the MNF method vary with different block numbers into which the ground samples were segmented.

without PC transform are the same, which means that PC transform is not impacted by the spatial distribution of pixels. However, the OAs of classification results descends dramatically with the increasing number of mixed blocks when MNF transform is used. This experiment demonstrated that spatial distribution of pixels impacts both the fea-

3.2 Classification experiments using the improved MNF

From the analysis shown above, one can conclude that, if estimated NCM is precise, classification result from MNF transform may be better than that from PC transform. However, NCM estimation is badly affected by spatial distribution of pixels. To test the influence of the spatial distribution of pixels on the classification OA with the improved MNF method, the experiments in section 3.1 were performed again. Here, the results of the 12th experiments shown in Figure 6(a) are used to illustrate the advantage of the improved MNF transform.

In this experiment, ground objects are completely mixed. The eigenvalue curves of the classical and improved MNF method are listed in Figure 5. The ratio of the eigenvalues corresponding to low-level principle components to those corresponding to high-level principle components in the new method is much higher than the ratio in the classical method, which means that the first few bands in the improved MNF can extract the features of different ground objects more effectively. Figure 6 shows MNF transform results and classification results with classical and improved NCM estimation methods. Figure 6(a) is the original hyperspectral image in which ground objects of the same class were divided into 12 blocks. Figure 6(b) is the classical MNF transform result displayed with the first 3 bands. Figure 6(c) is the improved MNF transform result. We can see that the colors of different ground objects can be differentiated more easily in 6(c), such as rock M1 and M2. From the classification results shown in Figure 6(d) and (e), it is obvious that the classification image in 6(e) from the improved method achieves better overall accuracy than the image in 6(d) when they are compared with Figure 6(f).
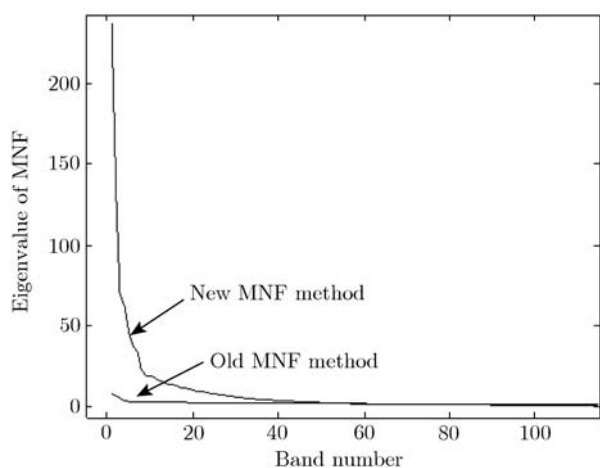

Figure 5 Eigenvalue curves of MNF transform using the old noise-estimation method and the improved one when the block number is 12. Different samples are mixed sufficiently.

The robustness of the improved MNF method against the spatial distribution of pixels is also proven using similar experiments in section 3.1. The OA curve of the improved MNF transform method is shown in Figure 7. Although the OA curve of classical MNF transform is higher than the curve of the improved method in the beginning cases where the corresponding images are relatively homogenous, the OA values of the improved method become much higher and more stable than those with the classical method when the mixing levels is increasing. The overall accuracy of classification with the improved MNF transform method does not descend very much at the end of the curve.

3.3 Application of the improved MNF

In this experiment, the real hyperspectral image, push-broom hyperspectral imager (PHI) data acquired in Minamimaki of Japan is used to illustrate the advantage of the improved MNF transform method. The PHI imager was developed by the Shanghai Institute of Technical Physics, China. The data used here is radiance hyperspectral data with 80 bands from 400 to 850 nm. A region shown in Figure 8(a) with mixing ground objects is chosen as the test image. The image size is 144 high by 195 wide. There are seven types of ground objects in it, including Japanese cabbage, Chinese cabbage, lettuce, grazing, ground film, wet soil and dry soil. Their spectra are shown in Figure 8(c) with different colors corresponding to the colors of ground object in the ground truth image shown in Figure 8(b). It can be seen from Figure 8(a) that different types of ground object are dispersed and mixed together, and the number of selected bands is larger than that of object types. The classified map treated as the ground truth image in Figure 8(b) is obtained by a feature-optimized expert decision-making classification method with some artificial modifications and was verified by field surveys in Minamimaki, Japan. Therefore, this classified map is used as the reference for evaluating classification results in this experiment[19,20]. It can be seen from Figure 8(c) that wet soil, dry soil and ground film can be easily distinguished, but it is difficult to distinguish the four types of vegetations. Eight different classification experiments were conducted with the different combinations of image transform methods, ROI samples selection or spectral band selection (see Table 1).

The PCA, MNF and improved MNF transform methods are used to compress spectral information
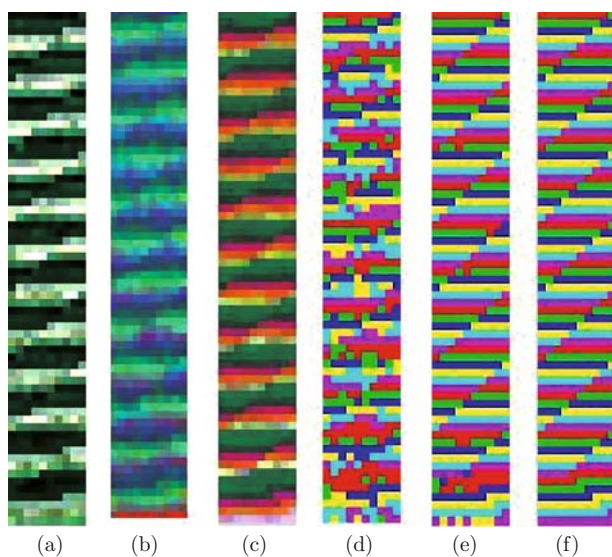
Figure 6 (a) Original hyperspectral image; (b) MNF transforms results using the old NCM estimation method; (c) MNF transforms results using the improved NCM estimation method; (d) classification results using the old MNF method; (e) classification results using the improved MNF method; (f) ground truth image.
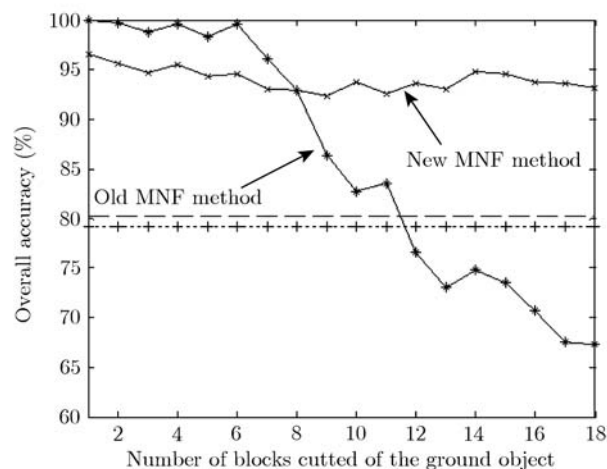
Figure 7 Comparisons of the classification OA using MNF transform with old and improved NCM estimation.
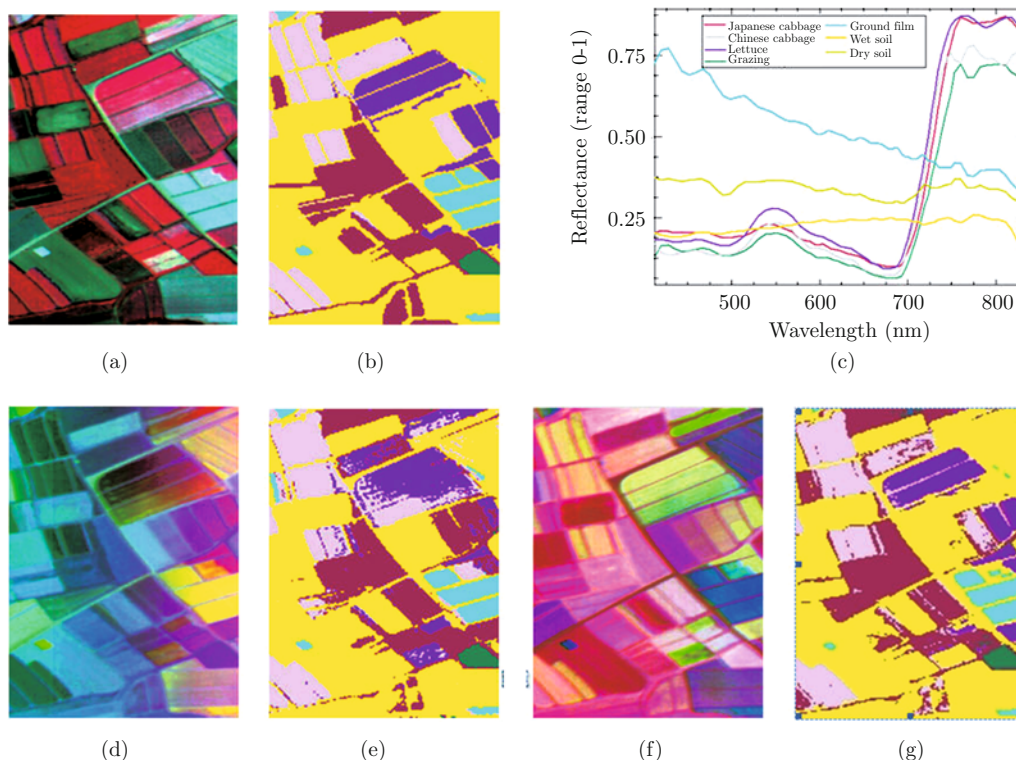

Figure 8 Classification results of crops on the PHI image. (a) Infrared color image of reflectance combined by bands 80, 42 and 19, 2% linear stretch displayed; (b) approximately correct classification result; (c) spectral curves of 7 sorts of typical ground objects; (d) combined display of first three components acquired by classical MNF transform; (e) classification result using classical MNF transform (5th experiment); (f) combined display of the first three principal components acquired by the improved MNF transform; (g) classification result using the improved MNF transform (8th experiment).

Table 1 Statistics of OA using different combinations

Sequence number	Transform method	ROI extraction method	Band/component selection	Classification accuracy	Kappa coefficient
1	No transform	Prior knowledge	80 bands	1.2963%	0.5725
2	PCA	PPI	Fore 9 components	71.2108%	0.5714
3	MNF	Prior knowledge	Fore 9 components	74.2949%	0.6039
4	MNF	PPI	Fore 9 components	75.2778%	0.5951
5	Improved MNF	Prior knowledge	Fore 9 components	76.2286%	0.6598
6	Improved MNF	PPI	Fore 9 components	85.9900%	0.7876
7	Improved MNF	PPI	Fore 30 components	86.1930%	0.7907
8	Improved MNF	PPI	Fore 50 components	86.2179%	0.7910

and separate noise before classification. The ROI used in classification is extracted through priori knowledges or the pure pixel index (PPI) method. Final classification results are evaluated using the overall accuracy (OA) and Kappa coefficient which are listed in Table 1. From Table 1 it is clear that the classification accuracies are approximately the same with and without the use of the PC transform, which proves that the PC transform can only compress spectral information. The accuracy result is improved obviously when the classical MNF transform method is used for classification. However, this improvement is not obvious due to the inaccurate NCM estimate for mixed ground objects.

It can be seen in Figure 8(d) that the classical MNF transform method treats noise caused by a heterogeneous array of sensors as signals in feature extraction. The classification result using the improved MNF transform method is shown in Figure 8(g). The classification accuracy is obviously improved when the improved MNF transform is used to extract features, especially when ground objects are completely mixed together. Because the improved MNF transform method uses the information of correlation between bands to estimate noise, it can also restrain the heterogeneous noise of the sensors in principal components. It should be noted from Figure 8(g) that most pixels at the ridge of field are mixtures of soil and vegetation. Classification results through any combinations are

not accurate in this place. How to get correct decisions on mixed pixels along the edge needs to be studied further.

4 Conclusions and discussion

This paper shows that Green and Berman's MNF transform can be used to compress data, separate noise and extract features for homogenous images. However, the spatial distribution of pixels affects this transform dramatically, and feature extraction results may not be used for classification when ground objects are mixed together. The theoretical reasons on this are illustrated. An improved MNF method is proposed to solve this problem, in which the NCM is estimated in both the spatial and spectral domains. Feature extraction results from this improved method are better than those from the classical MNF transform. This transform method can be used to compress data and separate noise effectively when the homogeneous blocks cannot be found in the whole image.

Experimental results from both simulated and real hyperspectral images in this study show the advantages of the improved MNF transform method. The algorithm complication of the improved MNF transform method for hyperspectral image needs to be reduced. The advantages of this method in other applications of the feature extraction field should be further studied.

1 Tong Q X, Zhang B, Zheng L F. Hyperspectral Remote Sensing. Beijing: Higher Education Press, 2006. 145–154

2 Keshava N, Mustard J F. Spectral unmixing. IEEE Signal Proc Exploit Hyperspect Imag, 2002, 19: 44–57

3 David G G, Andrew D, Niemann K O, et al. Processing HYPERION and ALI for forest classification. IEEE Trans Geosci Remote Sens, 2003, 41(6): 1321–1331

4 Jacob T M, Nancy F G, Keith T W, et al. Discrimination of hoary cress and determination of its detection limits via hyperspectral image processing and accuracy assessment techniques. Remote Sens Environ, 2005, 96(3-4): 509–517

5 Zhang B, Chen Z C, Zheng L F, et al. Object detection based on feature extraction from hyperspectral imagery and convex cone projection transform. J Infrared Millim W, 2004, 23(6): 441–445

6 Green A A, Berman M, Switzer P, et al. A transformation for ordering multispectral data in terms of image quality with implications for noise removal. IEEE Trans Geosci Remote Sens, 1988, 26(1): 65–74

7 James B L, Woodyatt A S, Berman M. Enhancement of high spectral resolution remote-sensing data by a noise-adjusted principal components transform. IEEE Trans Geosci Remote Sens, 1990, 28(3): 295–304

8 Nielsen A A. Analysis of regularly and irregularly sampled spatial, multivariate, and multi-temporal data. Dissertation for the Doctoral Degree. Lyngby: Institute of Mathematical Modelling, Technical University of Denmark, 1994. 45–74

9 Gao L R. Spectra enhancement and feature extraction for target detection in hyperspectral imagery. Dissertation for the Doctoral Degree. Beijing: Institute of Remote Sensing Applications, Chinese Academy of Science, 2007. 40–70

10 Conradsen K, Nielsen B K, Nielsen A A. Noise removal in multichannel image data by a parametric maximum noise fractions estimator. In: Proceedings of the 24th International Symposium on Remote Sensing of Environment, Rio de Janeiro, Brazil, 1991. 403–416

11 Olsen S I. Estimation of noise in images: an evaluation. Graph Model Image Proc, 1993, 55(4): 319–323

12 Roger R E. Principal components transform with simple, automatic noise adjustment. Int J Remote Sens, 1996, 17(14): 2719–2727

13 Roger R E, Arnold J F. Reliably estimating the noise in AVIRIS hyperspectral images. Int J Remote Sens, 1996, 17(10): 1951–1962

14 Gao L R, Zhang B, Zhang X, et al. A new operational method for estimating noise in hyperspectral images. IEEE Geosci Remote Sens Lett, 2008, 5(1): 83–87

15 Curran P J, Dungan J L. Estimation of signal-to-noise: a new procedure applied to AVIRIS data. IEEE Trans Geosci Remote Sens, 1989, 27(5): 620–628

16 Gao B C. An operational method for estimating signal to noise ratios from data acquired with imaging spectrometers. Remote Sens Environ, 1993, 43(1): 23–33

17 Corner B R. Noise estimation in remote sensing imagery using data masking. Int J Remote Sens, 2003, 24(4): 689–702

18 Greco M, Diani M, Corsini G. Analysis of the classification accuracy of a new MNF based feature extraction algorithm. In: Proceedings of SPIE. International Society of Optical Engineering, Stockholm, Sweden, 2006. V6365

19 Zhang B, Chen Z C, Zheng L F, et al. Object detection based on feature extraction from hyperspectral imagery and convex cone projection transform. J Infrared Millim W, 2004, 23(6): 441–445

20 Zhang B, Jia X P, Chen Z C, et al. A patch-based image classification by integrating hyperspectral data with GIS. Int J Remote Sens, 2006, 27(15): 3337–3346